Wave Absorption Profile during ICRF Heating in Mixed Plasma in Large Helical Device*)

Hiroshi KASAHARA, Tetsuo SEKI, Kenji SAITO, Dimitry MOSEEV[1)], Naoto TSUJII[2)], Goro NOMURA and Motonari KANDA

National Institute for Fusion Science, Toki 509-5292, Japan
[1)]*Max-planck Institute for Plasma Physics, Greifswald, 17491, Germany*
[2)]*University of Tokyo, Kashiwa 277-0882, Japan*

(Received 16 January 2023 / Accepted 26 June 2023)

A minority ion ratio in fast wave heating for the ion cyclotron range of frequencies affects plasma heating mechanisms and mode conversion ratios to short waves in a mixed plasma. The mode conversion region and these wave absorption profiles are functions of minority ion ratio, and direct wave absorption by electrons increases when the minority ion ratio exceeds about 6% in a simple two-dimensional wave absorption calculation with a single toroidal mode. At the minority ion ratio of 10%, the amount of absorption by electrons is comparable to that by ions. We find a significant relationship between the minority ion ratio and the wave absorption profile, exceeding the minority ion ratio of 10% for wave absorption to electrons.

Keywords: fast wave, short-wavelength, minority ion ratio, wave calculation

DOI: 10.1585/pfr.18.2402065

1. Introduction

Minority ion heating with the ion cyclotron range of frequency (ICRF) waves is an attractive plasma heating method to increase the temperature at plasma ignition phase in a reactor. Optimized minority ion ratio in two-ion species plasma is approximately 3 - 5%. However, the ion ratio in the reactor is supposed to be deuterium (D): tritium (T) = 50:50, and it is far from an optimized minority ion ratio in two-ion species plasmas. To realize plasma heating in a reactor using ICRF waves, a three-ion minority heating scheme with an ion ratio of D:T: beryllium (Be) = 55:45:0.01 is suggested [1]. A three-ion minority heating scheme has been demonstrated in JET, Alcator C-Mod, and ASDEX Upgrade, and the heating efficiencies were comparable to the two-ion minority heating scheme. Since these schemes are associated with minority ion ratio near ICRF resonance, the minority ion ratio strongly affects the plasma heating profile.

Wave-particle interaction for ICRF heating was studied in a mixed plasma. The experimental results were evaluated using full-wave calculations such as AORSA [2], TASK/WM [3], or single-pass absorption calculations with the assumption for simple wave propagations, which are based on a Fourier transformed hot plasma dispersion relation with a single parallel wavenumber to a magnetic field line in torus plasmas. Considering the calculation results, the optimized ion ratio for minority heating in tokamaks was a few percent [4, 5], but it was difficult to demonstrate the optimized minority ion ratio in actual plasma experiments, because impurity contaminations could not be negligible from the first wall and divertor, made by high Z materials.

In complex magnetic configurations like the Large Helical Device (LHD) [6], the optimized minority ion ratio using a simple two-dimensional wave calculation was a few percent [7] for ICRF heating scenarios. After repeated long-pulse discharge cleaning, an extremely low minority ion ratio could be achieved with a similar level to the optimized minority ion ratio for ICRF heating in the LHD. Since a single-pass absorption in the LHD with complex three-dimensional cyclotron resonance is relatively lower than that in tokamaks with simple resonance geometry, for energetic particle studies, it is essential to optimize the minority ion ratio to obtain a relatively high single-pass absorption. In a low hydrogen ratio below 10% for deuterium plasmas, the minority ion ratio did not always seem to agree between the measurement and the prediction from wave heating results. We could not get apparent peak heating efficiency below the minority ion ratio of 10% from the actual plasma experiments, but the dependence for heating efficiency was consistent with the prediction from wave absorption for the ion ratio exceeding 10% [7].

This is one of the long-standing mysteries of ICRF heating in the LHD. The line integrated sight of spectroscopy to measure a minority ion ratio passes the plasma center at the poloidal cross-section [8], and passes two ICRF resonances in different horizontal positions in sight. Spectroscopy and ICRF antennas [9, 10] are installed in

author's e-mail: kasahara.hiroshi@nifs.ac.jp
*) This article is based on the presentation at the 31st International Toki Conference on Plasma and Fusion Research (ITC31).

different toroidal sections, and the toroidal distance between the spectroscopy and the gas puff for minority ion fueling is more than twice as far from the gas puff to the ICRF antenna. Since the spectroscopy is sensitive to the signal intensity at the plasma edge, the thickness of the scrape-off layer at the plasma edge [11] may affect the evaluation of the minority ion ratio for the spectroscopy. Since we assume no profiles for minority ion ratio in toroidal and radial directions, the discrepancy of the minority ion ratio between the measurement and the heating prediction may be caused by the profile assumption, too.

Minority ion ratio in mixed plasma strongly affects the distances between an ion-ion hybrid resonance layer (IIH), an L-cutoff layer (L), and an ion cyclotron resonance layer (Ω_i), and it changes the primary wave absorption mechanism and profiles with the increases in minority ion ratio. A finite element method (FEM) has been studied with complex geometries for the structure of the ICRF antenna and the vacuum vessel surface to reveal wave propagation and the absorption profiles of electrons and ions. Although there are many challenges in solving the hot plasma dispersion relation for calculating wave propagation and absorption profiles [12], a lower hybrid wave calculation was demonstrated in the LEAF [13] with the hot plasma dielectric tensor in the integral formula. In this integral formula, a direct electron heating component is implemented for the electron Landau damping mechanism, and other heating mechanisms have not yet been used. Since it is still difficult to establish the hot plasma dielectric tensor in the integral formula for the ICRF heating in the LHD, we made a simple electric field calculation framework with an axisymmetry, combining the original hot plasma tensor and the commercial FEM solver with the frequency domain in the poloidal plasma cross-section.

In this paper, we introduce that wave absorption for an ICRF minority heating scheme is very sensitive to the minority ion ratio in the LHD. In the second section, we describe a simple wave calculation framework for the FEM and many assumptions to implement the calculation of wave absorptions. In the third section, we show the electric field of left and right-hand circularly polarized components on the poloidal cross-section. Finally, in the fourth section, wave absorption profiles for ions and electrons are shown and summarized in various minority ion ratios in the LHD.

2. A Simple Wave Calculation

We make a simple wave calculation framework to evaluate the wave propagation and absorption profile on the poloidal cross-section coordinate (R, ϕ, Z) in front of the ICRF antenna. The poloidal cross-section coordinates R, and Z are in radial and vertical directions, and the ϕ is the toroidal direction, in which the axisymmetry is the Z axis. The electric fields are calculated by combining the original hot plasma dielectric tensor module and a commercial solver (COMSOL Multiphysics with its RF module for a frequency domain [14]). The solution for huge sparse matrices with a triangular mesh with a single toroidal mode on an axisymmetric axis was calculated using the Multifrontal Massively Parallel sparse direct solver (MUMPS) in the COMSOL. The wave dispersion relation for determining the wave electric field is as follows.

$$\begin{aligned}
&\nabla \times (\nabla \times \nabla \vec{E}) - \frac{\omega^2}{c^2} \overline{\overline{K}}_c \cdot \vec{E} = i\mu_0 \omega \vec{J_{ext}}, \\
&\overline{\overline{K}}_c = R_t(-\theta_1) \cdot R_t(-\theta_2) \cdot \overline{\overline{\epsilon}}_{\text{hot, stix}} \cdot R_t(\theta_2) \cdot R_t(\theta_1), \\
&\overline{\overline{\epsilon}}_{\text{hot, stix}} = \overline{\overline{\epsilon}}_{\text{prop}} + i\overline{\overline{\epsilon}}_{\text{absorp}} \sim \overline{\overline{\epsilon}}_{\text{hot, stix k}_0}, \\
&\vec{E}(R, \phi, Z) = \vec{E}(R, Z)\, e^{-im\phi},
\end{aligned} \tag{1}$$

where $\vec{E}$, $\vec{J_{ext}}$, ω, $\overline{\overline{K}}_c$, $\overline{\overline{\epsilon}}_{\text{hot, stix}}$, m, μ_0, ϵ_0 and c are the electric fields, the external currents, the angular wave frequency of the launching wave, the hot plasma dielectric tensor, its translated dielectric tensor on the Stix frame, the toroidal mode number of the launching wave, the vacuum permeability and permittivity, and the light speed. The rotational matrixes R_t transform the electric field from the (R, ϕ, Z) coordinate to the Stix frame using two rotational angles of θ_1 and θ_2. The $\overline{\overline{\epsilon}}_{\text{hot, stix}}$ consists of a wave propagation compornent of $\overline{\overline{\epsilon}}_{\text{prop}}$ and a wave absorption compoenent of $\overline{\overline{\epsilon}}_{\text{absorp}}$. For cold plasma, the $\overline{\overline{\epsilon}}_{\text{prop}}$ is a cold plasma dielectric tensor, and the $\overline{\overline{\epsilon}}_{\text{absorp}}$ is zero because there is no wave absorption.

The electric fields $\vec{E}(R, \phi, Z)$ with three-dimensional components are calculated in the plasma region with the plasma dielectric tensor and in the vacuum region with vacuum condition. As a boundary condition for the wall and the antenna structures, stainless steel for the surface material is adopted, implementing Joulse losses. Although only a single toroidal mode limits the parallel component of the electric field, the parallel wavenumber associated with the toroidal mode number is varied on the poloidal cross-section with the assumption of mode conservation. We assume the primary launching wavenumber is associated with the current strap geometry of the ICRF antenna, and the parallel wavenumber of k_0 to the magnetic field line at the ICRF antenna position is set to $5.82\,\text{m}^{-1}$ in this model.

In previous works using the FEM frameworks, the hot plasma dielectric tensor associated with the wave propagation component of $\overline{\overline{\epsilon}}_{\text{prop}}$ is approximated by the cold plasma dielectric tensor of $\overline{\overline{\epsilon}}_{\text{cold, stix}}$ in the LEAF [15], and we agree on the assumption except for the ICRF resonance position because $\overline{\overline{\epsilon}}_{\text{cold, stix}}$ has an infinity issue on ICRF resonance position for ICRF waves. The wave absorption component $\overline{\overline{\epsilon}}_{\text{absorp}}$ for the hot plasma tensor is implemented for electron heating for electron Landau damping, which is mainly the heating mechanism in a lower hybrid wave. It is an integral formula in various parallel numbers by integral convolution techniques [15].

However, the hot plasma dielectric tensor for the integral formula for the LEAF is insufficient for the wave

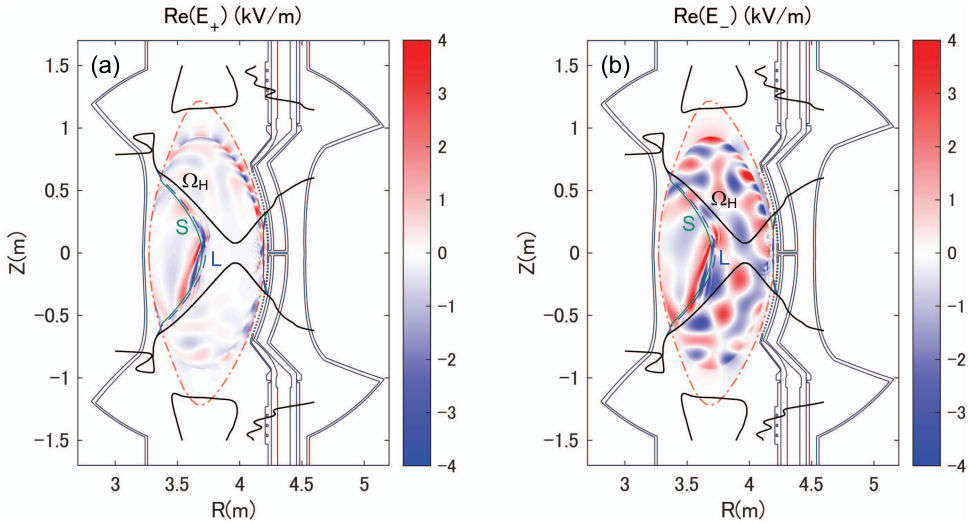

Fig. 1 Electric fields for left and right-hand circularly polarized components (a) and (b) with parallel wavenumber 5.82 m^{-1} for launching wave at ICRF antenna position in D(H) plasma with assumption of hydrogen ratio of 12%. Other plasma parameters were used from experimental results at timing of 4.75 sec in LHD discharge of SN164152. Typical positions for Stix notations for hydrogen cyclotron resonance (Ω_H), ion-ion hybrid resonance (S), and L cut-off layer (L) are shown.

absorption component because the harmonics cyclotron damping is relatively strong compared to electron Landau damping for wave absorption using the ICRF heating in the mixed plasma. Since it is reported that the plasma heating efficiency evaluated from diamagnetic energy with the amplitude modulation of ICRF power agrees with the wave absorption using a Fourier-transformed hot plasma dispersion relation with a single toroidal mode on the poloidal cross-section [7], we used a hot plasma tensor $\overline{\overline{\epsilon}}_{\mathrm{hot,\,stix\,k_0}}$ with a single parallel wavenumber as a substitute for the hot plasma tensor $\overline{\overline{\epsilon}}_{\mathrm{hot,\,stix}}$ in the FEM calculations.

To get the hot plasma dielectric tensor $\epsilon_{\mathrm{hot,\,k_0}}$ on the poloidal cross-section, we calculated the perpendicular wavenumbers using an initial perpendicular wavenumber from the solution for the cold plasma dispersion relation. The hot plasma dispersion relation, with a Maxwellian velocity distribution, includes cyclotron damping below the harmonic number of 10th and Landau damping and transit time magnetic pumping for a single parallel wavenumber; and there are several solutions for perpendicular wavenumbers for the hot plasma dispersion relation with the single parallel wavenumber. We selected the perpendicular wavenumber from a solution with an initial perpendicular wavenumber in the order of fast wave, slow wave, and electrostatic wave, where they could exist. Although using this technique, the propagatable wave was smoothly connected from the launching wave to the other waves in the plasma region; we neglected high-order electrostatic waves because there was no good resolution to include the high-order electrostatic wave in this calculation framework. With this assumption, the $\overline{\overline{\epsilon}}_{\mathrm{hot,\,stix}}$ in equation (1) was approximated by the $\overline{\overline{\epsilon}}_{\mathrm{hot,\,stix\,k_0}}$ evaluated by a single parallel wavenumber and the perpendicular wavenumber for its solution.

3. Electric Fields in a Mixed Plasma

Figure 1 shows the electric field profiles while launching the fast wave with a frequency of 38.47 MHz from the ICRF antenna at the radius of 4.2 m with the uniform wave current of 50 A/m on the strap surface as a wave source with a hydrogen ion ratio r_H of 12% as an assumption in the mixed plasma for D, H, He ions in the LHD. We used the plasma and magnetic configurations in an LHD discharge of SN164152 at 4.75 s, except for a minority ion ratio. Although we were able to use the ion ratios of H, He, and D measured by the spectrometer, we used the hydrogen ratio r_H as a control parameter for the minority ion ratio. Since quasi-neutral conditions were broken with the artificial hydrogen ratio, those conditions were satisfied by adjusting the ion ratio of the deuterium ions. Charge exchange spectroscopy and Thomson scattering gave the ion temperature, electron temperature, and electron density profiles. The magnetic field configuration was (B, R_{ax}, γ, B_q) = (2.75 T, 3.6 m, 1.254, 100%) [6], and the magnetic fields of (B_r, B_ϕ, B_z) in the plasma region were obtained from a best-fit profile, comparing the equilibrium by the VMEC code [16] and the pressure profile using Thomson scattering data [17]. The ion and electron temperature profiles were parabolic, with central temperatures of 1.8 keV and 4 keV, and the electron density profile was hollow with $1.4 \times 10^{19} m^{-3}$ at the plasma center and $2 \times 10^{19} m^{-3}$ at the normalized minor radius of ρ of 0.6.

These circularly polarized components of the electric fields are strongly associated with (a) slow waves for the left-hand circularly polarized component E_+ and with (b) fast waves for the right-hand circularly polarized component E_- in Fig. 1. Up and down asymmetry appears in both electric fields for the vertical direction, and significant electric field strength for the E_+ exists near the center

of the plasma and close to the IIH layer (S) with short-wavelength waves. In previous works on the comparison of the perpendicular wavenumbers between the measurement and calculation in tokamak experiments [18], it is reported that the ion cyclotron wave (ICW) and the ion Bernstein wave (IBW) are connected to fast waves in the higher magnetic field region around the IIH layer. They can appear as a short-wavelength mode in the E_+, which is associated with the IBW, as seen in Fig. 1 (a). In Fig. 1 (b), the fast wave, designed as a launching wave, has good accessibility in the plasma region, and there is no short-wavelength mode like Fig. 1 (a) with the inverse sign of the electric field strength.

This simple wave calculation shows the absorption region for the E_+ between the ion-ion hybrid resonance and the ion cyclotron damping layers. The estimated absorption region is consistent with the previous work [7] with the two-dimensional wave calculation with uniform electric field amplitude. In this simple wave calculation, the profile of electric field strength can be determined by boundaries of the vacuum vessel and the ICRF antenna. An adequate electric field strength profile can be provided compared to the previous work. As the hydrogen ion ratio increases, the distances between an ion-ion hybrid resonance layer, an L-cutoff layer, and an ion cyclotron resonance layer become longer. The primary wave absorption mechanism changes from ion cyclotron damping to ion cyclotron damping and electron Landau damping in the r_H of 1 - 10%.

Figure 2 shows the wave absorption profiles with various minority ion ratios in (a) electron and (b) ion for ICRF heating, and Fig. 3 shows (a) the maximum absorbed power densities and (b) their peak positions in various minority ion ratios. The magnetic configuration and plasma parameters are the same as those used for Fig. 1, except for the minority ion ratio. Figure 2 shows characteristics of wave absorption profiles and one or two peaks in various hydrogen ratios. With the r_H below 3%, these absorption profiles for electrons are broad, as seen in such as Fig. 2 (a), and the peak power densities for electrons are much lower than that for ions, as seen in Fig. 3 (a). The primary heating mechanism for the r_H below 6% is ion cyclotron damping, and these wave absorption of ions are dominant. Because finite Larmor radius effects are weak with applied plasma parameters, harmonic cyclotron damping is not strong compared to electron Landau damping with the r_H below 0.1%. Finally, the amount of wave absorption for electrons with the r_H below 0.1% was not large, and electron damping could not be negligible in an extremely low minority ion ratio. Summarizing the peak positions for wave absorption in the various minority ion ratios, the movement direction for these peak positions changed from inward to outwards for the normalized minor radius with the increase in the minority ion ratio. The minimum positions for the normalized minor radius are 3% for ions and 10% for electrons.

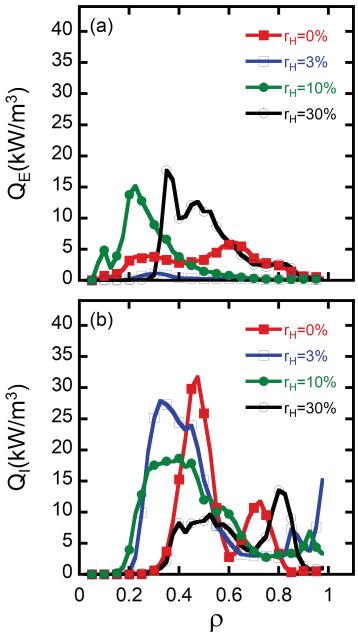

Fig. 2 Absorption profiles of electrons (a) and ions (b) for normalized radius (ρ) in various hydrogen ratios (r_H) of 0 - 30%.

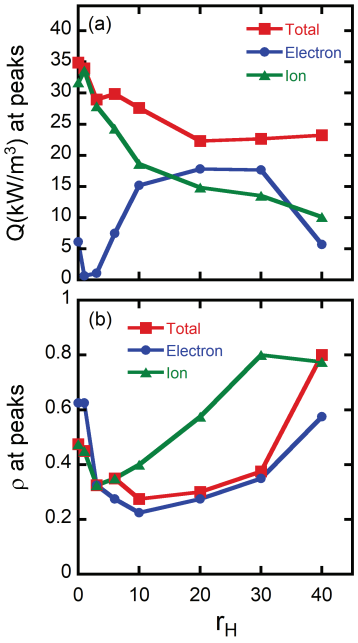

Fig. 3 Peak absorption power densities (a) and their positions (b) for total and electrons and ions in various hydrogen ratios (r_H) of 0 - 40%.

4. Summary and Discussion

The finite element method helps the evaluation of wave propagation and absorption, including the actual structure inside the vacuum vessel, but there are many challenging works to establish the integral formula for the dielectric hot plasma tensor, including the wave absorption mechanism considering the plasma kinetic theory.

We devised a simple wave calculation framework on the toroidal symmetry model on the FEM, combining the commercial electric field solver and the original hot plasma dielectric tensor to study the wave absorption profile with various minority ion ratios, and the hot plasma tensor was estimated by a perpendicular wavenumber, given from a solution of the Fourier transformed hot plasma dispersion relation, using a single parallel wavenumber. Since the experimental plasma heating efficiency and wave absorption using a two-dimensional calculation with the Fourier transformed hot plasma dispersion relation with a single parallel wavenumber are consistent [7], we consider the calculation of wave absorption is not far off the experimental wave absorption.

This simple calculation framework shows the two electric fields for left and right-hand circularly polarized components in the plasma region with the r_{H} of 12%. Although these existing regions in the plasma are consistent with the predictions from the previous simple wave calculation, the presence of short-wavelength waves around IIH layers with the r_{H} of 12% in a minority heating scenario for ICRF in the LHD is a new finding because the minority ion ratio is relatively small for mode-converted wave heating scenario.

In the mixed plasma in the LHD, a simple wave calculation tells us that as the minority ion ratio increases, the primary heating mechanism changes from cyclotron damping and electron Landau damping to electron Landau damping, exceeding the r_{H} of 10%. The peak position of wave absorption by electrons moves inward in the normalized radius until the minority ion ratio increases to 10%, moving outward as the minority ion ratio increases. When the minority ion ratio is 0.1 - 3%, the absorption power density of the electrons is extremely low compared to that of ions because ion cyclotron damping is dominant. In extremely low minority ion ratio, the r_{H} below 0.1%, the broad wave absorption profile for electrons is achieved, because the amount of wave absorption by electron Landau damping is close to that by ion cyclotron damping with the small finite Larmor radius. In focusing on wave absorption of electrons in a minority ion ratio exceeding 10%, significant absorption peaks of electrons appear, and they are associated with the position of the IIH layer, which is shifted outwards with the increase of minority ion ratio.

Acknowledgement

The authors thank the LHD experiment group for their excellent support in getting experimental plasma profiles, and this work is supported by the National Institute for Fusion Science Grant administrative budgets (NIFS22ULRR703) and JSPS KAKENHI Grant Number JP16K06944. The LHD data can be accessed from the LHD data repository at “https://www-lhd.nifs.ac.jp/pub/Repository_en.html.”

[1] Ye.O. Kazakov, J. Ongena, J.C. Wright, S.J. Wukitch *et al.*, Phys. Plasmas **28**, 020501 (2021).
[2] E.F. Jaeger, R.W. Harvey, L.A. Berry, J R. Myra, R.J. Dumont, C.K. Phillips *et al.*, Nucl. Fusion **46**, S397 (2006).
[3] A. Fukuyama *et al.*, FEC 1-6 Nov. Villamoura (Portugal) **20**, TH/P2-3 (2004).
[4] Y. Lin, J.C. Wright and S.J. Wukitch, J. Plasma Phys. **86**, 5, 865860506 (2020).
[5] L.F. Lu, B. Lu, X.J. Zhang, L. Colas *et al.*, Nucl. Fusion **63**, 066023 (2023).
[6] M. Osakabe, H. Takahashi, H. Yamada, K. Tanaka *et al.*, Nucl. Fusion **62**, 042019 (2022).
[7] S. Kamio, K. Saito, R. Seki, H. Kasahara *et al.*, Nucl. Fusion **62**, 016004 (2022).
[8] M. Goto, S. Morita, H.Y. Zhou and C.F. Dong, Fusion Sci. Technol. **58**, 394 (2010).
[9] H. Kasahara, T. Seki, K. Saito, R. Seki *et al.*, Phys. Plasmas **21**, 061505 (2014).
[10] K. Saito, T. Seki, H. Kasahara, R. Seki *et al.*, Fusion Eng. Des. **96-97**, 583 (2015).
[11] M. Kobayashi, S. Morita, C.F. Dong, Z. Cui *et al.*, Nucl. Fusion **53**, 033011 (2013).
[12] K. Miyamoto, Research Report NIFS PROC Series **88**, 310-316 (2011).
[13] O. Meneghini, S. Shiraiwa and R. Parker, Phys. Plasmas **16**, 090701 (2009).
[14] Multiphysics, COMSOL, COMSOL Multiphysics, Burlington, MA, accessed Feb **9**, 2018 (1998).
[15] S. Shiraiwa, O. Meneghini, R. Parker, P. Bonoli *et al.*, Phys. Plasmas **17**, 056119 (2010).
[16] S.P. Hirshman and J.C. Whitson, Phys. Fluids **26**, 3553 (1983).
[17] C. Suzuki, K. Ida, Y. Suzuki, M. Yoshida *et al.*, Plasma Phys. Control. Fusion **55**, 014016 (2013).
[18] E. Nelson-Melby, M. Porkolab, P.T. Bonoli, Y. Lin *et al.*, Phys. Rev. Lett. **90**, 155004 (2003).